



Published in final edited form as:

Nat Med. 2009 January ; 15(1): 104–109. doi:10.1038/nm.1854.

Selective molecular imaging of viable cancer cells with pH-activatable fluorescence probes

Yasuteru Urano^{1,2,*}, Daisuke Asanuma¹, Yukihiro Hama³, Yoshinori Koyama³, Tristan Barrett³, Mako Kamiya¹, Tetsuo Nagano¹, Toshiaki Watanabe⁴, Akira Hasegawa⁴, Peter L. Choyke³, and Hisataka Kobayashi^{3,*}

¹ Graduate School of Pharmaceutical Sciences, The University of Tokyo, 7-3-1 Hongo, Bunkyo, Tokyo 113-0033, JAPAN

² PRESTO, Japan Science and Technology Agency, 3-5 Sanbancho, Chiyoda, Tokyo 102-0075, JAPAN

³ Molecular Imaging Program, Center for Cancer Research, National Cancer Institute, NIH, Bldg. 10, Room 1B40, MSC 1088, 10 Center Dr., Bethesda, MD 20892-1088, USA

⁴ Molecular Diagnostic Technology Group, Advanced Core Technology Department, Research and Development Division, Olympus Corporation, 2-3 Kuboyama-cho, Hachioji, Tokyo 192-8512, JAPAN

* To whom correspondence should be addressed. urano@mol.f.u-tokyo.ac.jp, (Y.U.), kobayash@mail.nih.gov (H.K.).

Authors' present contact address

Yasuteru Urano; Graduate School of Pharmaceutical Sciences, The University of Tokyo, 7-3-1 Hongo, Bunkyo, Tokyo 113-0033, JAPAN, PRESTO, Japan Science and Technology Agency, 3-5, Sanbancho, Chiyoda, Tokyo 102-0075, JAPAN, urano@mol.f.u-tokyo.ac.jp

Daisuke Asanuma; Graduate School of Pharmaceutical Sciences, The University of Tokyo, 7-3-1 Hongo, Bunkyo, Tokyo 113-0033, JAPAN, ff087001@mail.ecc.u-tokyo.ac.jp

Yukihiro Hama; Department of Radiology, National Defense Medical College, 3-2 Namiki, Tokorozawa, Saitama 359-8513, JAPAN, yjhama2005@yahoo.co.jp

Yoshinori Koyama; Department of Diagnostic and Interventional Radiology, Gunma Univertisy Hospital, 3-39-15 showa-machi, Maebashi, Gunma 371-8511, JAPAN, onoff@showa.gunma-u.ac.jp

Tristan Barrett; Department of Radiology, Addenbrooke's Hospital, Cambridge University Teaching Hospitals NHS Foundation Trust, Hills Road, Cambridge, CB2 2QQ, UK, tristan.barrett@googlegmail.com

Mako Kamiya; Graduate School of Pharmaceutical Sciences, The University of Tokyo, 7-3-1 Hongo, Bunkyo, Tokyo 113-0033, JAPAN, makokamiya@gmail.com

Tetsuo Nagano; Graduate School of Pharmaceutical Sciences, The University of Tokyo, 7-3-1 Hongo, Bunkyo, Tokyo 113-0033, JAPAN, tlong@mol.f.u-tokyo.ac.jp

Toshiaki Watanabe; Molecular diagnostic technology Group, Advanced Core Technology Department, Research and Development Division, Olympus Corporation, 2-3 Kuboyama-cho, Hachioji, Tokyo 192-8512, JAPAN, toshiaki_watanabe@ot.olympus.co.jp

Akira Hasegawa; Molecular diagnostic technology Group, Advanced Core Technology Department, Research and Development Division, Olympus Corporation, 2-3 Kuboyama-cho, Hachioji, Tokyo 192-8512, JAPAN, a_hasegawa@ot.olympus.co.jp

Peter L. Choyke; Molecular Imaging Program, Center for Cancer Research, National Cancer Institute, NIH Bldg. 10, Room 1B40, MSC 1088, 10 Center Dr., Bethesda, MD 20892-1088, USA, pchoyke@mail.nih.gov

Hisataka Kobayashi; Molecular Imaging Program, Center for Cancer Research, National Cancer Institute, NIH Bldg. 10, Room 1B40, MSC 1088, 10 Center Dr., Bethesda, MD 20892-1088, USA, Kobayash@mail.nih.gov

Author Contributions

Y. U.: planning the projects, developing the probes, perform the in vivo experiments, writing and editing papers

D. A.: developing the probes, perform the in vivo experiments, writing and editing papers

Y. H.: perform the in vivo experiments, writing and editing papers

Y. K.: perform the in vivo experiments, writing and editing papers

T. B.: perform the in vivo experiments, writing and editing papers

M. K.: developing the probes, perform the in vivo experiments, writing and editing papers

T. N.: planning the projects, writing and editing papers

T. W.: perform the in vivo experiments, writing and editing papers

A. H.: perform the in vivo experiments, writing and editing papers

P. L. C.: planning the projects, writing and editing papers

H. K.: planning the projects, perform the in vivo experiments, writing and editing papers

Abstract

It is a long-term goal of cancer diagnosis to develop tumor-imaging techniques that have sufficient specificity and sensitivity. To achieve this goal, minimizing the background signal originating from non-target tissues is critical. Here, we achieve highly specific *in vivo* cancer visualization by employing a newly-designed targeted “activatable” fluorescent imaging probe. This agent is activated after cellular internalization by sensing the pH change in the lysosome. Novel acidic pH-activatable probes based on the BODIPY fluorophore were synthesized, and then conjugated to a cancer-targeting monoclonal antibody. As proof of concept, *ex* and *in vivo* imaging of HER2-positive lung cancer cells in mice were performed. The probe was highly specific for tumors with minimal background signal. Furthermore, because the acidic pH in lysosomes is maintained by the energy-consuming proton pump, only viable cancer cells were successfully visualized. The design concept can be widely adapted to cancer-specific cell-surface-targeting molecules that result in cellular internalization.

Genetic cell labeling techniques show the possibility of detecting or tracing a single cell *in vivo*¹⁻³, however, currently available injectable molecular imaging probes are limited in their ability to detect small volumes of viable cancer because of low target-to-background ratios. Generally, small molecular probes lack specificity and low target accumulation, in contrast, larger molecules show prolonged high retention and background⁴. However, such large-molecular complexes are cleared slowly, so a considerable amount of unbound probe remains. These pharmacokinetic characteristics result in high background signal (Scheme 1a).

In order to overcome this problem, we developed an activatable fluorescence probe consisting of: 1) a cancer targeting macromolecule and 2) a small-molecular fluorescent moiety activated only within cancer cells to minimize the background signal and maximize tumor-to-normal tissue (T/N) ratio (Scheme 1b).

We targeted the human epidermal growth factor type 2 (HER2) receptor with the monoclonal antibody, trastuzumab which, after binding to HER2, is internalized *via* the endosomal-lysosomal degradation pathway⁵.

The lysosome is distinct from other cellular organelles because of its low pH (pH 5–6) relative to the cytoplasm (pH ~7.4). By designing a probe that activates in an acidic environment, the agent yields a highly tumor specific signal with greatly reduced background signal (Scheme 1c).

Results

Development of tunable, acidic pH-activatable fluorescent moiety

To achieve signal activation within the acidic environment of the lysosome, we required small-molecular fluorescent molecules with the following characteristics: 1) They should be almost non-fluorescent in the extracellular environment, *i.e.* at pH 7.4. 2) They should become highly fluorescent under acidic conditions, *i.e.* pH < 6. 3) They need to be excited by long-wavelength light (≥ 500 nm) and emit a fluorescent signal which overcomes autofluorescence. 4) They must covalently bind to the targeting ligand or antibody. 5) They must be tunable to different pKa values for maximizing the T/N ratio. For developing probes, the concept of photoinduced electron transfer (PeT) was employed. Briefly, if a chemical substrate reacts specifically with the target analyte and if its HOMO or LUMO energy level changes dramatically upon reaction, a fluorescence probe can be developed for the analyte by conjugating the substrate with an appropriate fluorophore⁶⁻⁹.

In order to develop a series of acidic pH-sensitive fluorescence probes suitable to tag proteins, we selected anilines as the reactive moiety towards protons, and 2,6-dicarboxyethyl-1,3,5,7-tetramethylBODIPY as a fluorophore¹⁰. BODIPYs are well known to show strong emission over 500 nm, and their fluorescence is unaffected by solvent polarity and pH. Further, 2,6-dicarboxyethyl-1,3,5,7-tetramethylBODIPY has two carboxylic groups which can be used for coupling to proteins. N,N-Dialkylated anilines have sufficiently high HOMO energy levels to cause PeT towards the BODIPY fluorophore, and substitution of the N-alkyl group causes a pKa shift, so that it should be possible to develop a series of pH-tunable compounds. Based on these strategies we developed a series of novel, acidic pH-sensitive fluorescence probes bearing various anilines at the 8-position of the BODIPY fluorophore. These compounds were almost non-fluorescent ($\Phi_{fl} < 0.002$) in the non-protonated form due to PeT from the aniline moiety to the fluorophore, but became highly fluorescent ($\Phi_{fl} = 0.55-0.60$) in the protonated form showing greater than 300-fold increase in emission (Fig. 1a, Supplementary Table 1 online). Figure 1b shows the pH-dependent changes in emission intensity of acidic pH-sensitive probes, as well as the constant emission from pH-independent “always on” BODIPY bearing benzene instead of aniline. The pKa values differed depending upon the alkyl group on the nitrogen, ranging from 3.8 to 6.0 as shown in Fig. 1c.

Next, we conjugated these fluorescence probes to trastuzumab by using their mono NHS ester derivatives to form an amide bond with Lys residues of the antibody. We selected conjugates with DOL (degree of labeling) = 2.7–3.0 as optimal, and evaluated their pH-dependent fluorescence emission intensity. The resultant probe-antibody conjugates produced acid-sensitive, reversible fluorescence (Fig. 1d, Supplementary Movie 1 online). The pKa values were 4.4, 4.9, and 5.8 for DiMeNBODIPY-, EtMeNBODIPY-, and DiEtNBODIPY-trastuzumab, respectively – almost identical to the values of the free probes.

In Vitro Imaging of HER2-positive Cells using a Targeted Activatable Probe

Fluorescence was confined to the plasma membrane on the image obtained immediately after addition of the “always on” control probe (Fig. 2a). After ≥ 2 hours, small bright spots appeared inside the cells, likely corresponding to endosomal uptake of the probe. These results demonstrate that the control probe shows strong fluorescence, regardless of its cellular location.

In contrast, almost no fluorescence was observed immediately after the addition of the pH-activatable probes (Fig. 2a). Because all probes were initially outside the cells at neutral pH, the probe was still almost non-fluorescent. After 2 hours, however, the probe conjugates were partially internalized by endocytosis, leading to the formation of endosomes. In the case of DiEtNBODIPY-trastuzumab, some fluorescent spots were observed within the cells, but not on the plasma membrane, presumably reflecting the lowered pH inside the endosomes. However, DiMeNBODIPY-trastuzumab and EtMeNBODIPY-trastuzumab produced few fluorescent spots inside the cells, suggesting that the environment of early endosomes is not sufficiently acidic to activate these compounds. After 4 hours, all activatable probes exhibited strongly fluorescent spots within the cells, which co-localized with LysoTracker dyes (Fig. 2b), and this activation lasted at least 1 day. These results demonstrated pH-dependent activation of the probe-conjugates, and only the cells that internalized these probes became fluorescent, whilst the background fluorescence was minimal. Among a series of activatable probes, DiEtNBODIPY-probe showed stronger signal than DiMeNBODIPY- and EtMeNBODIPY-probes, so we selected DiEtNBODIPY-trastuzumab as a pH-activatable agent for further *in vivo* tumor imaging experiments.

In vivo Imaging of HER2-positive Lung Metastases Using a Targeted Activatable Probe

In order to examine the potential of our approach for *in vivo* imaging, we performed *in situ* and *ex vivo* spectrally resolved fluorescence imaging of freshly resected lungs bearing metastatic

NIH/3T3 HER2 tumors with a control probe and a pH-activatable probe. As shown in Fig. 3a, the control probe produced signals from non-tumor-bearing lung tissue and the heart, whilst the pH-activatable agent only produced signals from HER2-positive tumors and the background fluorescence was suppressed. As a result, the tumor-to-heart ratio of the pH-activatable probe (DiEtNBODIPY-trastuzumab), which was calculated using 28 tumors of ~1 mm in diameter (254 ± 5 pixels), was 22-fold higher (193.0 vs 8.7 arbitrary unit, Supplementary tumor-to-heart ratio Table 2 online) than that of the control probe.

To confirm the specificity of this pH-activatable probe, a mixed metastatic lung tumor model of the HER2+/RFP- tumor cells and the constitutively expressed RFP in the HER2- cell line (RFP+/HER2-), were employed. The pH-activatable agent produced fluorescence only in HER2+/RFP- tumors, but not in RFP+/HER2- tumors, (Fig. 3b). In contrast, the control agent produced fluorescence not only in HER2+/RFP- tumors, but also in the surrounding tissues (Fig. 3b). Additionally, the control agent produced yellow fluorescence in the control RFP+/HER2- tumors, owing to the mixing of red and green probes in the blood pool and interstitium.

Sensitivity and specificity determinations were based on the evaluation of 22 mice with 940 tumors (468 and 472 with control and pH-activatable probes, respectively) with a size range between 0.5-2.0 mm. Comparison was made between RFP+/HER2- cell line and the BODIPY-based probe (green) targeting the HER2+/RFP- cell line. On green or red fluorescence unmixed images, all 940 tumors were visualized with either or both the green and red fluorescent signal (sensitivity 100% for both probes). Forty eight of 468 tumors examined in mice with the control probe and 3 tumors of 472 tumors examined in mice with the pH-activatable probe showed both green and red fluorescence (specificity 84.8 and 99.1% for control and pH-activatable probes, respectively, see also supplementary sensitivity/specificity Table 3).

In addition, a control humanized antibody, pH-activatable daclizumab against human IL-2 receptor α subunit¹¹, which has > 98% sequential homology to trastuzumab, did not demonstrate any fluorescence from the tumors (Fig. 3c).

In order to demonstrate that pH-activatable probes produce fluorescence only from living cells, cells or tumors were loaded with either control or pH-activatable agent, then treated with alcohol. Under fluorescence microscopy, the signal from pH-activatable probe-loaded cells disappeared immediately after addition of 30% ethanol, while the fluorescence signal from the control agent-loaded cells remained unchanged (Fig. 4a). Moreover, the signal in tumors, visualized with the pH-activatable agent, significantly decreased 30 min after dipping the tissues in ethanol ($p < 0.01$), whilst the signal in tumors visualized with the control agent, showed minimal change (Fig. 4b, c). The findings indicate that signal from pH-activatable probes reflects cell viability.

To demonstrate the versatility of the method, a peritoneal metastasis model of ovarian cancer in mice was targeted with galactosamine-conjugated serum albumin conjugated to the pH-activatable BODIPY. The *in vitro* and *in vivo* studies for detection and therapeutic monitoring of micro-metastasis performed with the HER2-targeted probe in the lung metastasis model were repeated for the ovarian cancer model (Supplementary Ovarian cancer figures 1-4). Furthermore, *in vivo* fluorescence micro-endoscopic experiments in live mice were performed to demonstrate that the method is amenable to a laparoscopic approach (Supplementary Fluorescence-guided laparoscope movies 2-4).

Discussion

Fluorescence-based probes have the advantage that their signal is potentially switchable depending on local conditions, and are now commonly used for visualizing cellular

processes¹². Nevertheless, few activatable fluorescence probes exist for *in vivo* imaging. Weissleder *et al.* developed activatable cyanine-based fluorescence probes based on cathepsin mediated dequenching, resulting in a 12-fold increase in signal^{13,14}. Our approach differs in that a macromolecule is used to target the probe, and activation occurs after internalization in the low pH environment of the lysosome. The fluorescence yield is higher and the process is reversible.

A few pH-sensitive fluorescence probes are commercially available, however, most are poorly suited to *in vivo* imaging because they activate with increasing pH¹⁵. Others activate under acidic conditions, but the wavelengths are too short¹⁶, or they are too hydrophobic and lack a tagging moiety for conjugation¹⁷, or their background signal under neutral pH conditions is relatively high¹⁸. The probes described here are almost non-fluorescent at neutral pH and highly fluorescent at acidic pH. This high sensitivity, combined with high specificity targeting, allows the selective detection and monitoring of viable cancer cells *in vivo*.

Another advantage of our probe is that activation is reversible, which enables the probe to produce signal only in viable cancer cells. Unlike previously reported irreversible activatable probes, our pH-activatable probes will lose signal upon leakage from the cell, as occurs with cell damage or death. Therefore, this method potentially permits real-time monitoring of therapy on living cancer cells¹⁹. In addition, this method could be useful to monitor the intracellular kinetics of receptor-ligand complexes.

Unlike other activatable probes^{13,20,21}, our DiEtNBODIPY-trastuzumab consists of two independently functioning components; a targeted macromolecule (monoclonal antibody or GSA) and a pH-sensitive small-molecular fluorescence probe which is tunable and activatable. Therefore, this method could employ any antibody or cytokine that is internalized after receptor-binding. In addition, not only can the pH-threshold of fluorescence be precisely tuned, but also the color (emission wavelength) can be changed by choosing different fluorophores such as rhodamines²² (Supplementary pH-activatable rhodamine Movie 5 online).

Trastuzumab has a high binding affinity for the cell surface marker, HER2/neu (erbB2/p185)²³ and therefore, could be potentially useful in HER2 expressing metastases^{24,25}. After forming homo-dimers, receptor-bound trastuzumab migrates to the lysosome as early as 45 min after binding²⁶, however, the internalization rate is ~4% of bound antibody per hour²⁷. Therefore, the use of more rapidly internalizing receptor-ligand systems including the D-galactose receptor system^{20,28} (Supplementary figures 1-4) could yield higher and earlier fluorescence signal. This agent could be adapted for clinical use with endoscopy or laparoscopy²⁹ and is potentially useful as an aid to surgery to improve completeness of resection³⁰.

In conclusion, we developed small-molecular pH-activatable fluorescence probes and targeted them to viable cancer cells using macromolecule conjugates. These probe conjugates can potentially be used as *in vitro* tools for evaluating intracellular receptor kinetics, cell viability and real-time monitoring of cell death, although their main potential application will be as a clinical tool for cancer detection and real-time monitoring of therapy.

Materials and Methods

Materials

General chemicals were of the best grade available, supplied by Aldrich Chemical Co., and Tokyo Chemical Industries, and Kokusan Chemical Works Ltd.

Antibodies

Trastuzumab, an FDA-approved humanized anti-human EGF receptor type 2 (HER-2) monoclonal antibody, which has a complimentary determination region (CDR) against an epitope of HER-2 grafted on a human IgG₁ framework, was purchased from Genentech Inc. (Herceptin®, South San Francisco, CA). Daclizumab, an FDA-approved humanized anti-human CD25 [IL-2 receptor α subunit, IL-2R α (Tac)] monoclonal antibody, which has a complimentary determination region (CDR) against an epitope of CD25 grafted on a human IgG₁ framework, was purchased from Hoffmann-La Roche Inc. (Zenapax®, Nutley, NJ).

Instruments

NMR spectra were recorded on a JEOL JNM-LA300 instrument at 300 MHz for ¹H NMR and 75 MHz for ¹³C NMR. Mass spectra were measured with a JEOL JMS-T100LC AccuToF. UV-visible spectra were obtained on a JASCO V-550. Fluorescence spectroscopic studies were performed on a JASCO FP-6500.

HPLC

Preparative HPLC was performed on an HPLC system composed of a pump (PU-2080, JASCO) and a detector (MD-2015, JASCO), with an Inertsil ODS-3 (10.0 mm × 250 mm) column (GL Sciences Inc.).

Fluorometric Analysis

The slit width was 3 nm for emission. The photomultiplier voltage was 300 V. Relative fluorescence quantum efficiency of BODIPY derivatives was obtained by comparing the area under the emission spectrum of the test sample excited at 490 nm with that of a solution of fluorescein in 0.1 N NaOH, which has a quantum efficiency of 0.850 according to the literature (*Analyst* 1960 85: 587-600. Correction of fluorescence spectra and measurement of fluorescence quantum efficiency. Paeker, C. A.; Rees, W. T.).

Cell Culture

NIH3T3/HER2+ and Balb3T3/HER2-/RFP+ cell lines (*Clin. Cancer Res.* 2007 May 15;13(10):2936-45. Spectral fluorescence molecular imaging of lung metastases targeting HER2/neu. Koyama Y, Hama Y, Urano Y, Nguyen DM, Choyke PL, Kobayashi H.) were grown in RPMI 1640 (GIBCO) containing 10 % fetal bovine serum (GIBCO), 100 U/mL penicillin, and 100 μ g/mL streptomycin at 37°C in humidified air containing 5% CO₂.

Labeling of Herceptin with BODIPY-mono-N-hydroxy-succinimidyl ester (NHS)

BODIPY-mono-NHS derivatives were dissolved in DMSO to obtain 10 mM stock solutions. Herceptin was incubated with BODIPY-mono-NHS in 200 mM sodium phosphate buffer, pH 8.4, at ambient temperature for 60 min in the dark. The BODIPY-Herceptin conjugate was separated from free BODIPY by using a PD-10 column (GE Healthcare) and PBS pH 7.4 (GIBCO) as the eluent. Assuming that the protein was obtained without any loss at the separation step, the degree of labeling ratio (DOL) (BODIPY [mol]/Herceptin [mol]) was determined by measuring the absorbance of the labeled Herceptin at 520 nm.

Confocal imaging of internalization of the BODIPY-labeled Herceptin into NIH3T3/HER2 cells

NIH3T3/HER2 cells were incubated on poly-(*l*)-lysine-coated dishes with RPMI 1640 without phenol red. A solution of BODIPY-labeled Herceptin in PBS pH 7.4 was added into the medium at a final concentration of 50 nM IgG. Confocal images were obtained at selected times using a U-LH100HG confocal laser scanning unit coupled to an IY81FVBF inverted microscope

with a PlanApo $\times 60$ objective lens (Olympus). The excitation wavelength was 488 nm and the emission was filtered using BA505IF filter.

Tumor model

All procedures were carried out in compliance with the Guide for the Care and Use of Laboratory Animal Resources (1996), National Research Council, and approved by the institutional Animal Care and Use Committee. The metastatic lung tumors were established by intravenous injection of 2×10^6 tumor cells suspended in 200 μL of PBS in 8-week-old female nude mice (National Cancer Institute Animal Production Facility, Frederick, MD, USA). Side-by-side comparative experiments with HER2+ lung metastatic tumor-bearing mice to directly compare “always on” with pH-activatable fluorophore-conjugated trastuzumab for specificity and living cell monitoring were performed at 19 days post-injection of 3T3/HER2+ cells. Two-color experiments with two injected cell lines of lung metastases in mice (RFP-transfected Balb3T3/HER2-/RFP+ and 3T3/HER2+) were conducted to evaluate the specificity of HER2+-expressing tumor detection were performed at 12 days (Balb3T3/HER2-/RFP+) and 19 days (3T3/HER2+) post-injection of cells. (Koyama 2007 CCR shown above)

Fluorescence imaging in mouse

Probes (50 nM as trastuzumab) in 0.066 M PBS was injected from the tail vein into the tumor-harboring mouse and left for 1 day. Then the mouse was anesthetized and sacrificed, followed by opening of the thorax. Fluorescence images in the thorax were captured with a Maestro™ In-Vivo Imaging System (CRI Inc., Woburn, MA, USA). The excitation wavelength was 480-520 nm, and emission spectra from 500 nm to 800 nm were obtained. Unmixed images were created with the use of authentic spectral patterns of the BODIPY, RFP, and the background (*Cytometry A*. 2006 Aug 1;69(8):748-58. Multispectral imaging in biology and medicine: slices of life. Levenson RM, Mansfield JR.).

Supplementary Material

Refer to Web version on PubMed Central for supplementary material.

Acknowledgments

This study was supported in part by the Precursory Research for Embryonic Sciences and Technology from JST Agency and by the research grants (Grant Nos. 19021010 and 19205021) to Y. U., and by the Intramural Research Program of the NIH, National Cancer Institute, Center for Cancer Research to H. K.

References

1. Yamamoto N, et al. Cellular dynamics visualized in live cells in vitro and in vivo by differential dual-color nuclear-cytoplasmic fluorescent-protein expression. *Cancer Res* 2004;64:4251–6. [PubMed: 15205338]
2. Yamauchi K, et al. Induction of cancer metastasis by cyclophosphamide pretreatment of host mice: an opposite effect of chemotherapy. *Cancer Res* 2008;68:516–20. [PubMed: 18199547]
3. Yang M, Jiang P, Hoffman RM. Whole-body subcellular multicolor imaging of tumor-host interaction and drug response in real time. *Cancer Res* 2007;67:5195–200. [PubMed: 17545599]
4. Wu AM, Senter PD. Arming antibodies: prospects and challenges for immunoconjugates. *Nat Biotechnol* 2005;23:1137–46. [PubMed: 16151407]
5. Yarden Y. The EGFR family and its ligands in human cancer. signalling mechanisms and therapeutic opportunities. *Eur J Cancer* 2001;37:S3–8. [PubMed: 11597398]
6. Miura T, et al. Rational Design Principle for Modulating Fluorescence Properties of Fluorescein-Based Probes by Photoinduced Electron Transfer. *J Am Chem Soc* 2003;125:8666–8671. [PubMed: 12848574]

7. Ueno T, et al. Rational Principles for Modulating Fluorescence Properties of Fluorescein. *J Am Chem Soc* 2004;126:14079–14085. [PubMed: 15506772]
8. Tanaka K, et al. Rational Design of Fluorescein-Based Fluorescence Probes. -Mechanism-Based Design of a Maximum Fluorescence Probe for Singlet Oxygen- *J Am Chem Soc* 2001;123:2530–2536. [PubMed: 11456921]
9. Urano Y, et al. Evolution of Fluorescein as a Platform for Finely Tunable Fluorescence Probes. *J Am Chem Soc* 2005;127:4888–4894. [PubMed: 15796553]
10. Gabe Y, Urano Y, Kikuchi K, Kojima H, Nagano T. Highly Sensitive Fluorescence Probes for Nitric Oxide Based on Boron Dipyrromethene Chromophore -Rational Design of Potentially Useful Bioimaging Fluorescence Probe- *J Am Chem Soc* 2004;126:3357–3367. [PubMed: 15012166]
11. Queen C, et al. A humanized antibody that binds to the interleukin 2 receptor. *Proc Natl Acad Sci U S A* 1989;86:10029–33. [PubMed: 2513570]
12. Minta A, Kao JPY, Tsien RY. Fluorescent Indicators for Cytosolic Calcium Based on Rhodamine and Fluorescein Chromophores. *J Biol Chem* 1989;264:8171–8178. [PubMed: 2498308]
13. Weissleder R, Tung CH, Mahmood U, Bogdanov A Jr. In vivo imaging of tumors with proteaseactivated near-infrared fluorescent probes. *Nat Biotechnol* 1999;17:375–378. [PubMed: 10207887]
14. Maeda H, Wu J, Sawa T, Matsumura Y, Hori K. Tumor vascular permeability and the EPR effect in macromolecular therapeutics: a review. *J Control Release* 2000;65:271–84. [PubMed: 10699287]
15. Paradiso AM, Tsien RY, Machen TE. $\text{Na}^+\text{-H}^+$ Exchange in Gastric Glands as Measured with a Cytoplasmic-Trapped, Fluorescent pH Indicator. *Proc Natl Acad Sci USA* 1984;81:7436–7440. [PubMed: 6095295]
16. de Silva AP, et al. Signaling Recognition Events with Fluorescent Sensors and Switches. *Chem Rev* 1997;97:1515–1566. [PubMed: 11851458]
17. Kollmannsberger M, Rurack K, Resch-Genger U, Daub J. Ultrafast Charge Transfer in Amino-Substituted Boron Dipyrromethene Dyes and Its Inhibition by Cation Complexation: A New Design Concept for Highly Sensitive Fluorescent Probes. *J Phys Chem A* 1998;102:10211–10220.
18. Adie EJ, et al. A pH-Sensitive Fluor, CypHer™ 5, Used to Monitor Agonist-Induced G Protein-Coupled Receptor Internalization in Live Cells. *Bio Techniques* 2002;33:1152–1154.
19. Nwokolo CU, Payne-James JJ, Silk DB, Misiewicz JJ, Loft DE. Palliation of malignant dysphagia by ethanol induced tumour necrosis. *Gut* 1994;35:299–303. [PubMed: 7512062]
20. Hama Y, et al. A Target-Cell Specific Activatable Fluorescence Probe for in vivo Molecular Imaging of Cancer based on a Self-Quenched Avidin-Rhodamine Conjugate. *Cancer Res* 2007;67:2791–2799. [PubMed: 17363601]
21. Kamiya M, et al. An Enzymatically Activated Fluorescence Probe for Targeted Tumor Imaging. *J Am Chem Soc* 2007;129:3918–3929. [PubMed: 17352471]
22. Hoffman RM. The multiple uses of fluorescent proteins to visualize cancer in vivo. *Nat Rev Cancer* 2005;5:796–806. [PubMed: 16195751]
23. Baselga J, Norton L, Albanell J, Kim YM, Mendelsohn J. Recombinant humanized anti-HER2 antibody (Herceptin) enhances the antitumor activity of paclitaxel and doxorubicin against HER2/neu overexpressing human breast cancer xenografts. *Cancer Res* 1998;58:2825–31. [PubMed: 9661897]
24. Gancberg D, et al. Comparison of HER-2 status between primary breast cancer and corresponding distant metastatic sites. *Ann Oncol* 2002;13:1036–43. [PubMed: 12176781]
25. Zidan J, et al. Comparison of HER-2 overexpression in primary breast cancer and metastatic sites and its effect on biological targeting therapy of metastatic disease. *Br J Cancer* 2005;93:552–6. [PubMed: 16106267]
26. Yarden Y. The EGFR family and its ligands in human cancer. signalling mechanisms and therapeutic opportunities. *Eur J Cancer* 2001;37:S3–8. [PubMed: 11597398]
27. Mandler R, Kobayashi H, Hinson ER, Brechbiel MW, Waldmann TA. Herceptin-geldanamycin immunoconjugates: pharmacokinetics, biodistribution, and enhanced antitumor activity. *Cancer Res* 2004;64:1460–7. [PubMed: 14973048]

28. Hama Y, Urano Y, Koyama Y, Choyke PL, Kobayashi H. D-galactose receptor-targeted in vivo spectral fluorescence imaging of peritoneal metastasis using galactosamin-conjugated serum albumin-rhodamine green. *J Biomed Opt* 2007;12:051501. [PubMed: 17994865]
29. Alencar H, et al. Colonic adenocarcinomas: near-infrared microcatheter imaging of smart probes for early detection--study in mice. *Radiology* 2007;244:232-238. [PubMed: 17507718]
30. De Grand AM, Frangioni JV. An operational near-infrared fluorescence imaging system prototype for large animal surgery. *Technol Cancer Res Treat* 2003;2:553-562. [PubMed: 14640766]

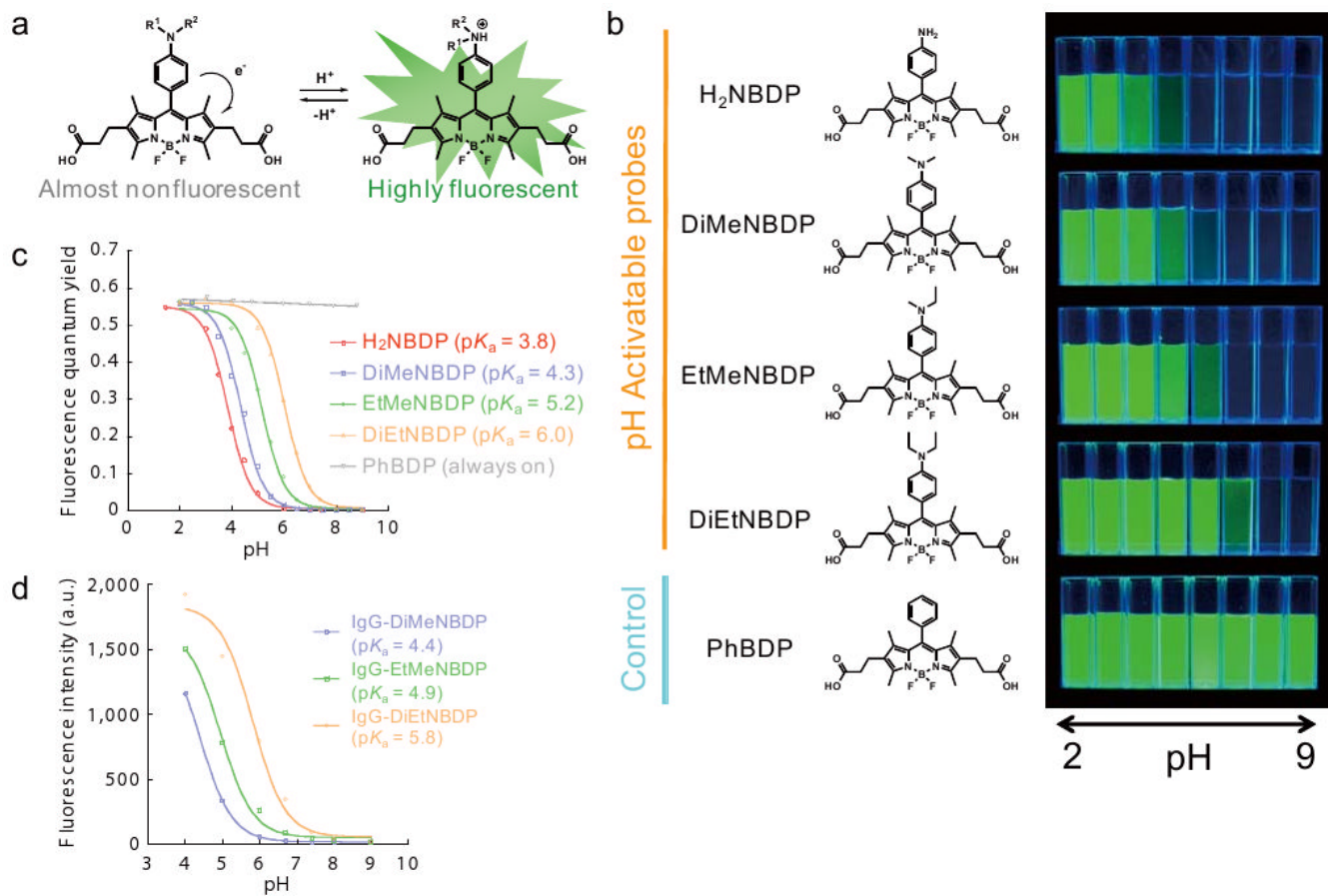


Figure 1. Development of a series of fluorescence probes for various acidic environments
(a) A scheme for the reversible and acidic pH-induced fluorescence activation of a probe. **(b)** pH profiles of fluorescence of H₂NBDP, DiMeNBDP, EtMeNBDP and DiEtNBDP as acidic pH-sensitive fluorescence probes, and PhBDP as a control “always on” probe. The pH ranges from pH 2 (left) to pH 9 (right) in one pH unit increments. **(c)** pH dependent changes in emission intensity of acidic pH-activatable BODIPY probes. Curve fitting was based on a modified Henderson-Hasselbach equation. **(d)** pH-dependent changes in emission intensity of acidic pH-activatable BODIPY-trastuzumab conjugates around the physiological pH range. DOL: PhBDP-IgG = 3.0, DiEtNBDP-IgG = 2.8, EtMeNBDP-IgG = 2.8, DiMeNBDP-IgG = 2.7

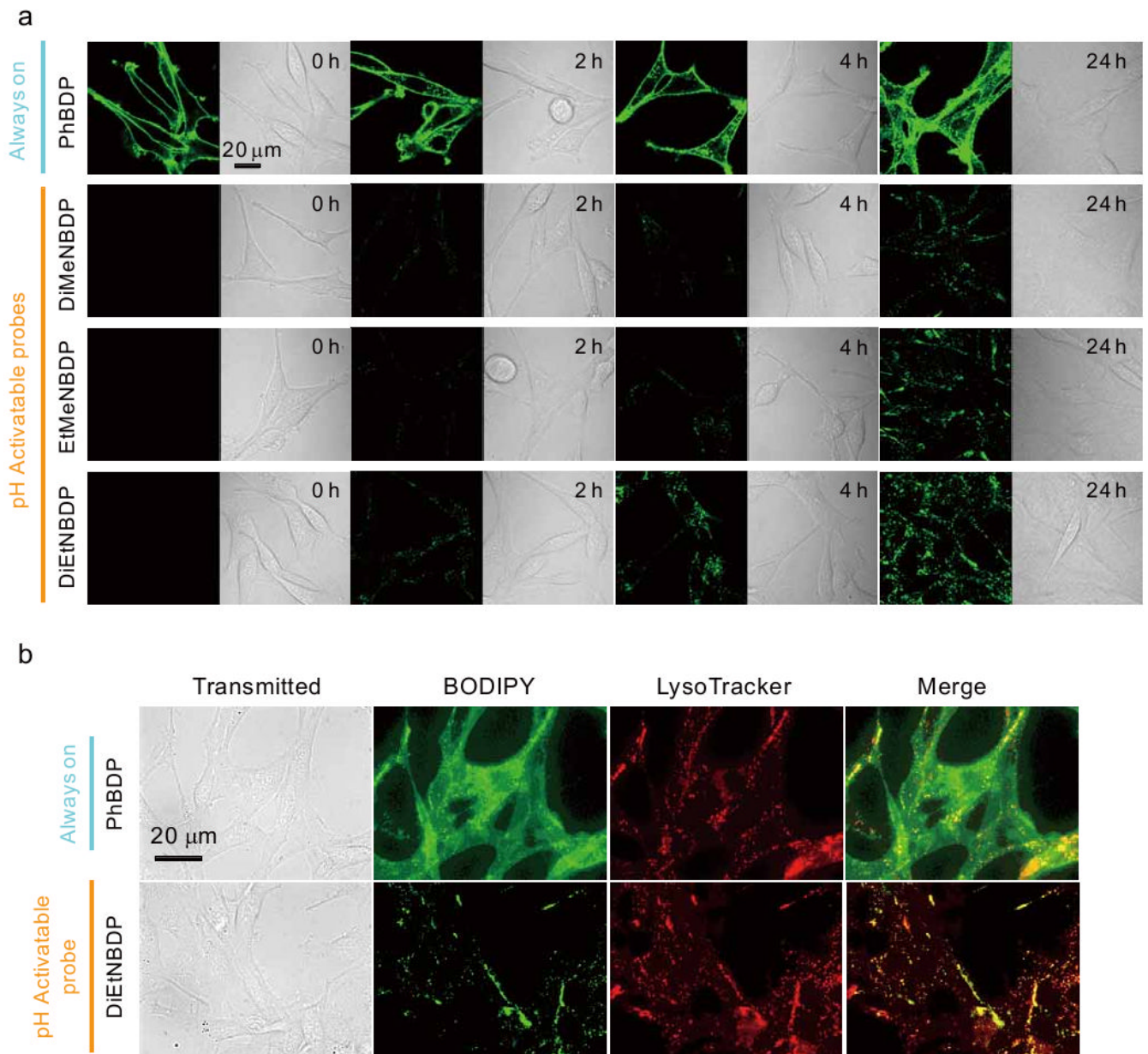


Figure 2. *In vitro* imaging of NIH3T3/HER2 cells with PhBODIPY-, DiMeNBODIPY-, EtMeNBODIPY- or DiEtNBODIPY-labeled trastuzumab

(a) Confocal microscope images of NIH3T3/HER2 cells obtained just after the addition of the probes, and at 2, 4, and 24 hours post-addition of BDP-conjugated trastuzumab to the medium.

(b) A solution of DiEtNBODP-, or PhBDP-conjugated Trastuzumab was added to NIH3T3/HER2 cells. Following incubation for 24 hr, LysoTracker Red DND-99 was added, and fluorescent images were obtained 1 hr post-addition of the organelle marker.

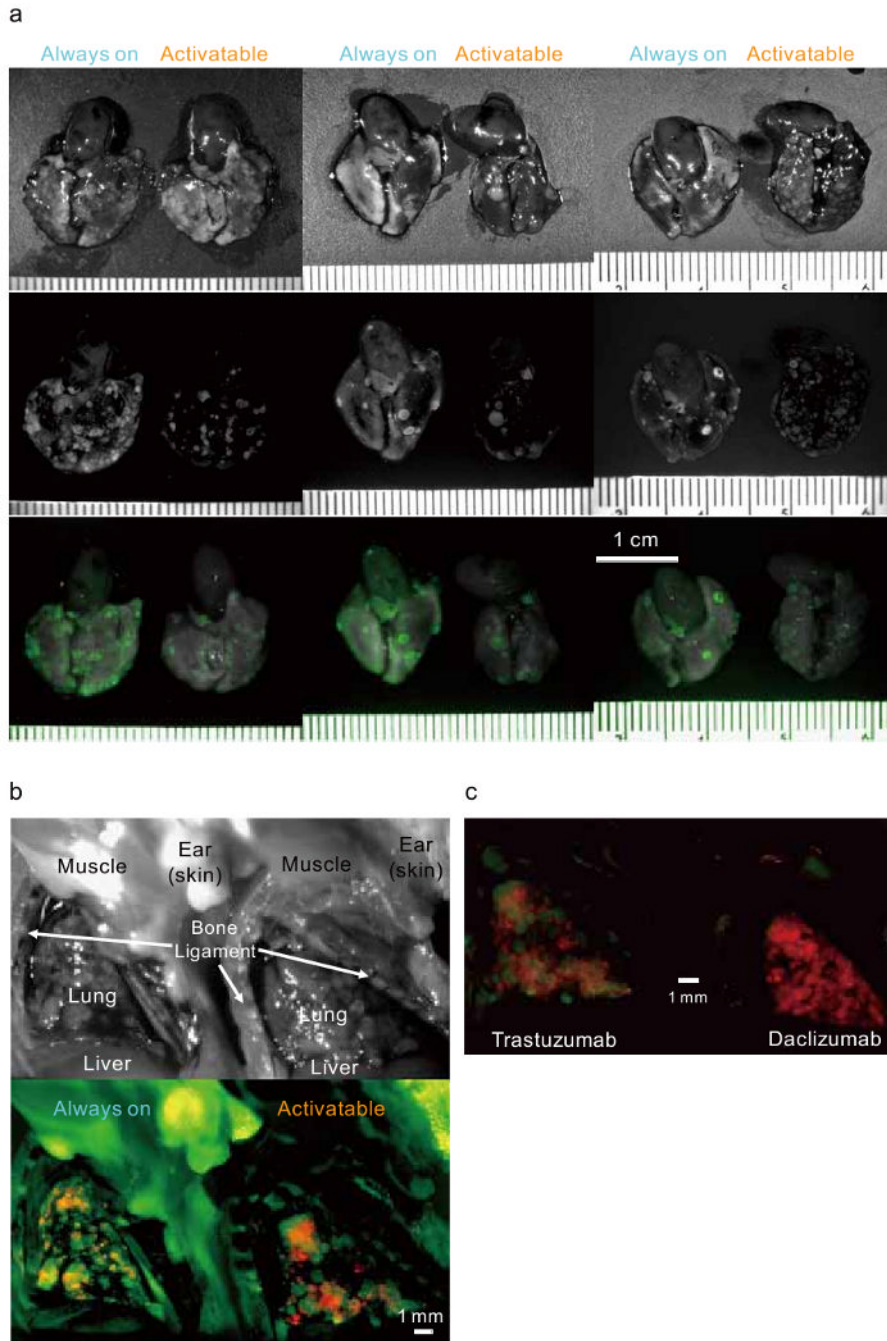


Figure 3. The activatable probe can produce a fluorescence signal only from HER2-positive tumors and not from HER2-negative tumors with minimal background from normal tissue
(a) White light (upper panel), spectrally unmixed green fluorescence (middle panel) and composite overlapped images (lower panel) of the lung one day after injection of always on (left) and activatable (right) optical imaging probes are shown. The activatable probe produces a fluorescence signal only from tumors in the lung, whilst the control “always on” probe produces a fluorescence signal not only from tumors, but also from the background normal lung and heart. The findings were observed consistently in all 8 sets of lungs examined. The first 3 consecutive sets of lungs are shown in the figure. **(b)** The activatable probe (bottom right) readily distinguishes HER2+ (green) and RFP+/HER2- (red) tumors in the lung. In

contrast, the control probe produces a green fluorescence signal not only from HER2+ tumors, but also from the normal background tissue and the RFP+/HER2- tumors - seen as yellow (a mixture of the green and red colors). Upper panel; White light images, Lower panel; spectrally unmixed and composite multicolor fluorescent images. (c) In the same mouse model as shown in (b), HER2-specific pH-activatable probe (trastuzumab; left) demonstrated HER2+ (green) and RFP+/HER2- (red) tumors in the lung, however, control pH-activatable humanized antibody (daclizumab, right) did not reveal any tumors. The normal tissue does not demonstrate fluorescence with either probe.

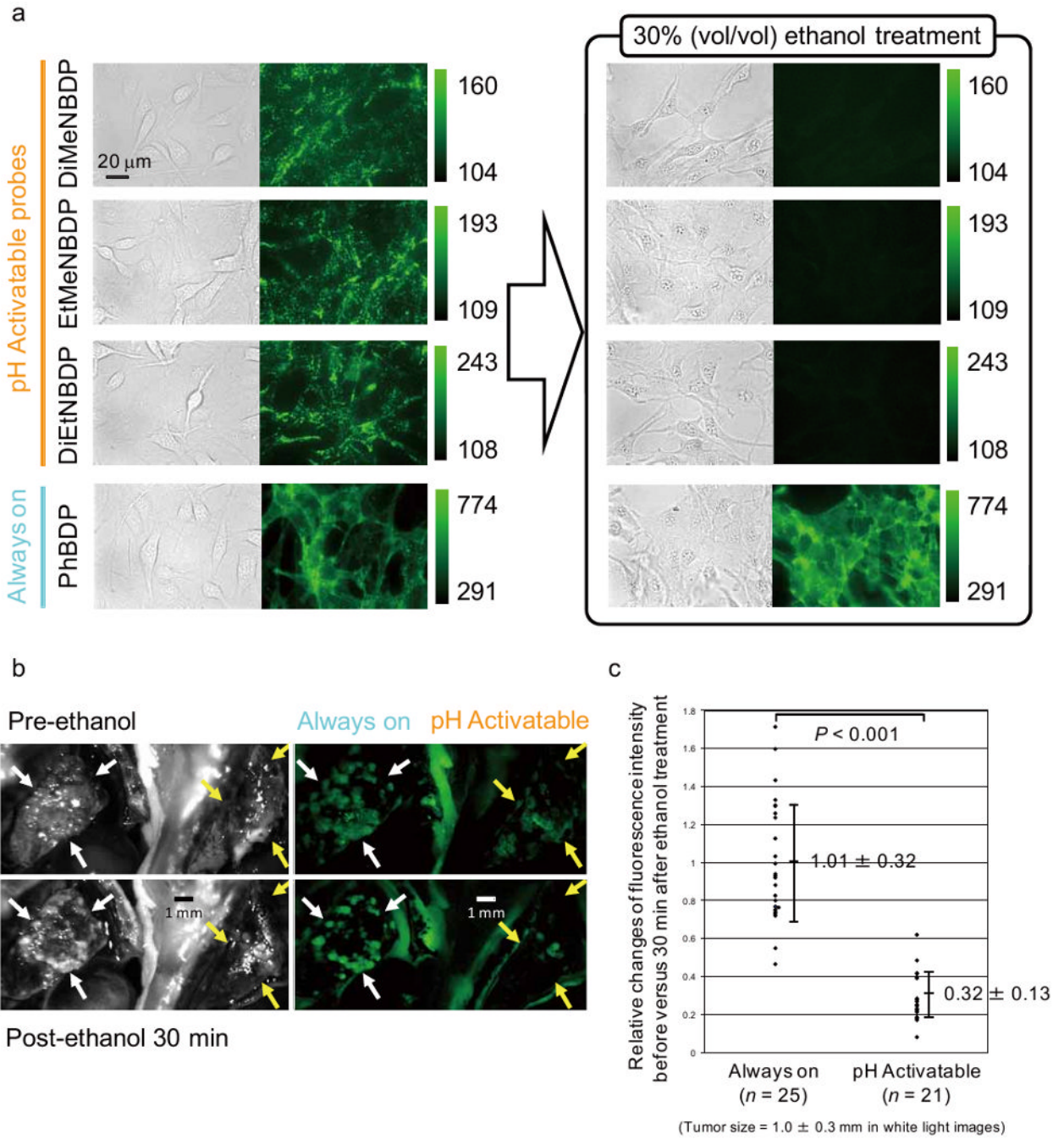
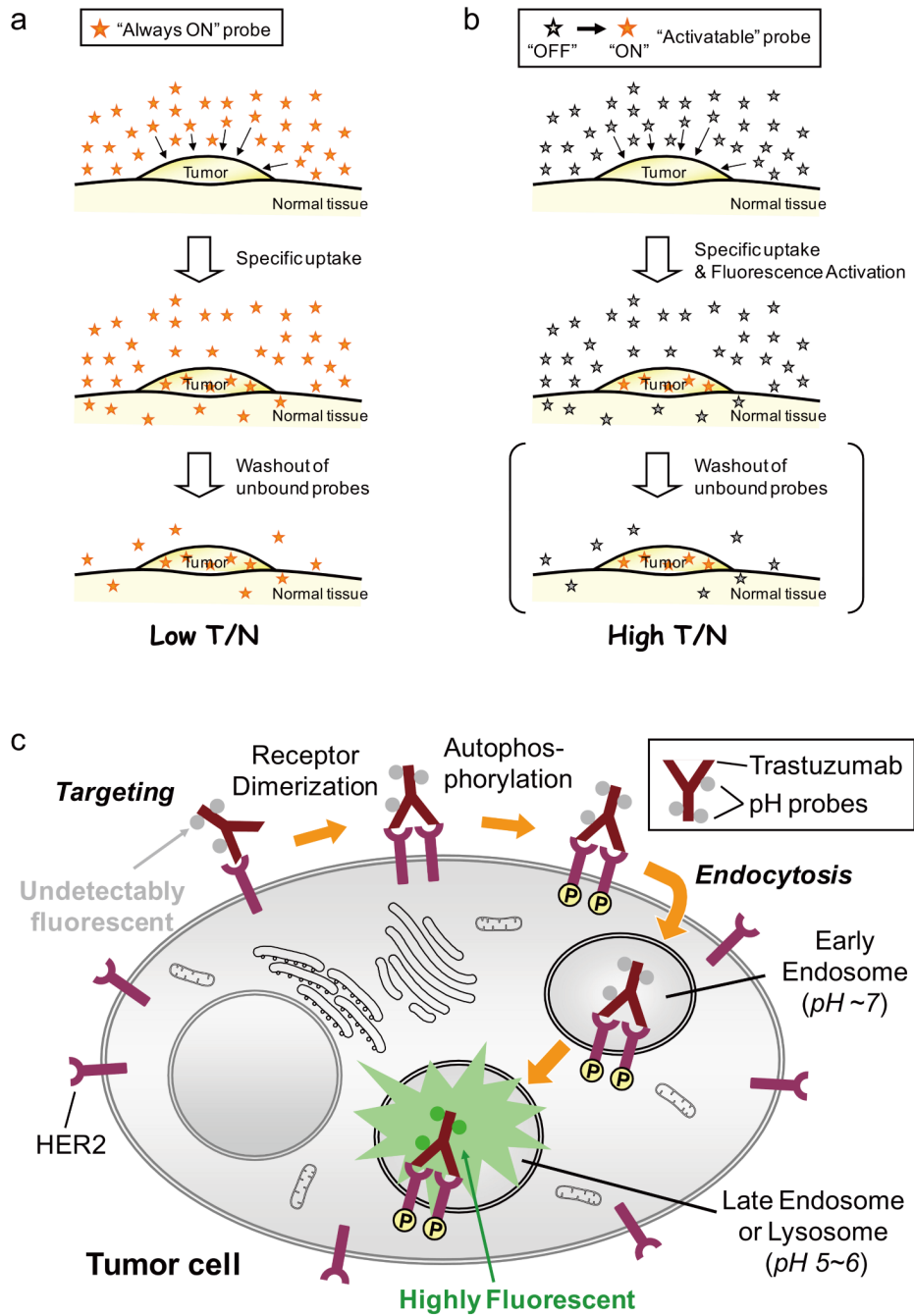


Figure 4. The activatable probe can produce a fluorescence signal only from living HER2-positive cells and tumors, and not from dead cells or fixed tumors

(a) Fluorescence and bright light images of NIH3T3/HER2 cells with PhBODIPY-, DiMeNBODIPY-, EtMeNBODIPY- or DiEtNBODIPY-labeled trastuzumab. Fluorescence images were obtained 5 hr after addition of the labeled trastuzumab (left), and then after treatment with 30% ethanol followed by 10-min incubation (right). (b) White light (left panels) and spectrally unmixed and composite fluorescence (right panels) images of lungs one day after *i.v.* injection of “always on” (left: white arrows) and activatable (right: yellow arrows) optical imaging probes and pretreatment (upper panels) or 30 min after dipping in the 100% ethanol (lower panels) are shown. The fluorescence signals from most of the small tumors,

visualized with the activatable probe (upper right) became almost invisible 30 min after dipping in 100% ethanol (lower right), while the fluorescence signals from most of the tumors loaded with the “always on” probe (upper left), were essentially unchanged. (c) Signal changes of individual surface tumors of 1.0 ± 0.3 mm in size before and after alcohol treatment were plotted. The fluorescence signals from most of the small tumors, which were visualized with the activatable probe (right), showed significant decrease in signal compared with those with the “always on” probe ($P < 0.01$).

**Scheme 1.**

(a) Existing strategies for tumor imaging with MRI, PET or non-activatable "always on" fluorescence detection. (b) Novel strategy for selective tumor imaging with activatable fluorescence probes. (c) A schematic representation of highly selective tumor imaging with an activatable fluorescence probe-antibody conjugate. The probe is non-fluorescent when outside the tumor cells. Following internalization by the endocytosis, the probe is accumulated in late endosomes or lysosomes, where the acidic pH activates the probe, making it highly fluorescent.